

Modulating Thermal Conductivity via Targeted Phonon Excitation

Xiao Wan,[▽] Dongkai Pan,[▽] Zhicheng Zong, Yangjun Qin, Jing-Tao Lü, Sebastian Volz, Lifa Zhang, and Nuo Yang*



Cite This: *Nano Lett.* 2024, 24, 6889–6896



Read Online

ACCESS |



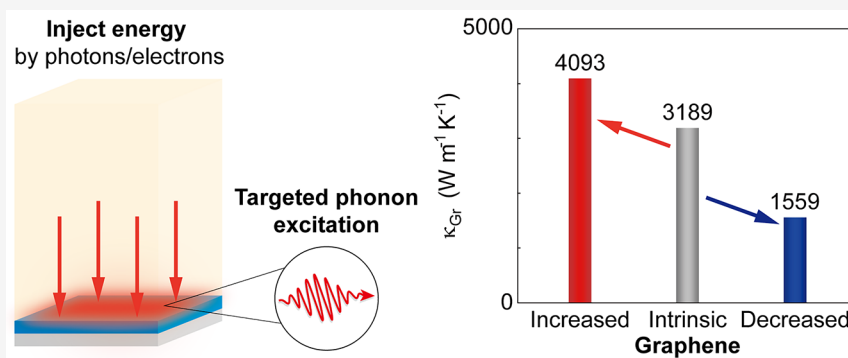
Metrics & More



Article Recommendations



Supporting Information



ABSTRACT: Thermal conductivity is a critical material property in numerous applications, such as those related to thermoelectric devices and heat dissipation. Effectively modulating thermal conductivity has become a great concern in the field of heat conduction. Here, a quantum modulation strategy is proposed to modulate the thermal conductivity/heat flux by exciting targeted phonons. It shows that the thermal conductivity of graphene can be tailored in the range of $1559 W m^{-1} K^{-1}$ (decreased to 49%) to $4093 W m^{-1} K^{-1}$ (increased to 128%), compared with the intrinsic value of $3189 W m^{-1} K^{-1}$. The effects are also observed for graphene nanoribbons and bulk silicon. The results are obtained through both density functional theory calculations and molecular dynamics simulations. This novel modulation strategy may pave the way for quantum heat conduction.

KEYWORDS: Thermal conductivity, Graphene, Graphene nanoribbon, Phonon

The modulation of thermal conductivity is of great importance in various applications, including thermal managements^{1–3} and energy devices.^{4–6} It means that thermal conductivity, as an intrinsic property of materials, can be enhanced or decreased by an external field. And then, the heat transfer characteristics of the material are altered. Achieving desirable performances requires a deep understanding of phonon scattering mechanisms in different heat transfer regimes, which is essential to modulate the thermal conductivity of materials.^{7–16} However, the complex nature of phonon transport has made the modulation of thermal conductivity a longstanding challenge in physics and material science.

Recent developments in the field of heat conduction have led to a better understanding of the scattering dynamics of heat carriers on the nanoscale. Heat conduction in dielectrics can be understood as the propagation of phonons and their scatterings such as phonon–phonon,^{17,18,20} impurity,^{21–23} and boundary scattering.^{9,24,25} Phonon–phonon scattering has been exploited to produce weaker couplings^{26–28} and to highlight hydrodynamic phonon transport^{11,29} in nanostructures. Impurity scattering is highly frequency dependent and is also closely related to normal processes,³⁰ which can redistribute

phonon frequencies and control phonon transport by nano-engineering.^{1,15,21,31,32} Due to size confinement, phonon transport is largely affected by the boundary scattering,⁹ resulting in the size dependence of thermal conductivity and leading to an invalid Fourier's law.^{33–35}

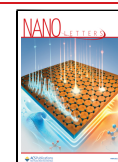
As the understanding of phonon scattering mechanisms has advanced, a variety of new strategies to modulate the thermal conductivity have been developed, motivated by the great demand for thermal management. An enhanced thermal conductivity can be achieved by minimizing phonon–phonon scattering phase space and phonon–impurity scattering in bulk materials.^{2,14,18–20,36–42} Conversely, to reduce thermal conductivity, the strategies that increase phonon scattering have been explored,^{43–46} such as intrinsically increasing anharmonicity or crystal complexity or extrinsically introducing disorder, defects, boundaries, interfaces, and nanoparticles.

Received: February 15, 2024

Revised: May 7, 2024

Accepted: May 7, 2024

Published: May 13, 2024



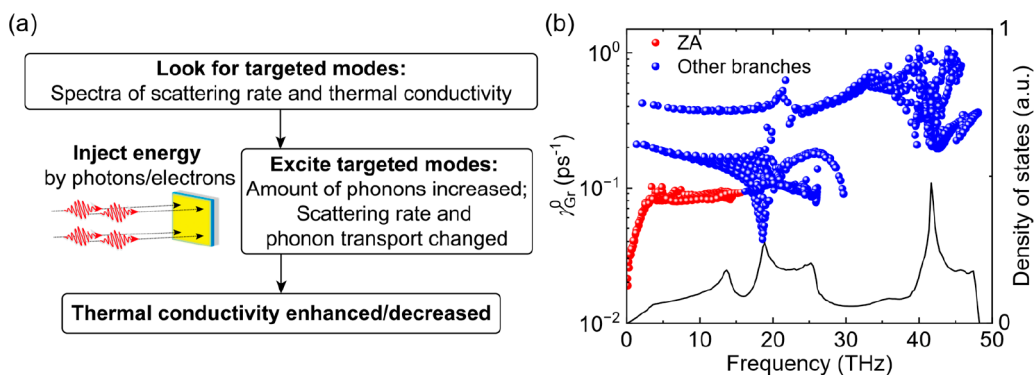


Figure 1. Modulating thermal conductivity via targeted phonon excitation. (a) Schematic of modulation strategy. (b) The density of states (DOS) and intrinsic scattering rates γ_{Gr}^0 of graphene (Gr) by ab initio calculations for choosing targeted phonons. The superscript “0” represents the intrinsic value.

Besides, the wave nature of phonons⁴⁷ can also be leveraged to modulate the thermal conductivity, as seen in the development of nanophononic crystals^{48–50} and the increase of tuning phonon coherence^{51–53} and localization.^{54–56} In recent works, external fields have been implemented to change the morphology of structures, thereby regulating thermal conductivity.^{37,41,57–59} Nevertheless, while these strategies mentioned above have shown promise, they currently cannot modulate the thermal conductivity with a mode targeting ability or controllability.

Recently, there has been growing interest in targeted phonon mode excitation using terahertz optical pulses or tensile strain to modulate optical and electrical properties. The methods offer several advantages such as in situ, flexibility, quick response, and directness, without requiring any structural modification. For instance, terahertz excitation pulses have been used to directly excite optical phonons in MAPbI₃, resulting in significant perturbations in the electron relaxation dynamics.⁶⁰ Similarly, selectively exciting vibrational modes of the molecules has been shown to modulate the performance of an organic optoelectronic system.⁶¹ Furthermore, the non-equilibrium carrier-phonon dynamics in photovoltaic systems have been discussed in detail for a few perovskites. These discussions have revealed the quantum emission of longitudinal optical (LO) phonons, the decay of optical phonons to acoustic phonons, and other relaxation processes when abundant carriers are injected.^{62–64} Nonequilibrium between optical and acoustic phonons has also been observed in photoexcited graphene and MoS₂.^{65,66} In black phosphorene, the excitation of out-of-plane acoustic phonons (ZA modes) induced by tensile strain can provide a strong modulation of the electronic band structures, carrier lifetime, and carrier mobility.⁶⁷ Additionally, targeted phonon excitation has been used to enhance ion diffusion⁶⁸ and induce structural phase transitions.^{69,70} While these results demonstrate the feasibility of targeted phonon excitation, fewer studies have investigated the strategy’s potential for modulating thermal conductivity.

Here, the strategy of quantum excitation of phonons is proposed to modulate the thermal conductivity of dielectric materials, where phonons dominate in the heat conduction. This strategy involves exciting targeted phonons to increase or decrease the phonon scattering, thus achieving the desired thermal conductivities. The effectiveness and capability of this strategy are demonstrated using ab initio calculations⁷¹ and molecular dynamics simulations.⁷² Graphene and graphene nanoribbon are chosen as the model systems, since the thermal

conductivities of graphene and its derivatives have been extensively studied. Besides, this strategy is also validated on typical 3D bulk silicon at 150 K (see Appendix A in the Supporting Information). The results indicate that the thermal conductivity can be modulated by exciting phonons in a quantum manner without altering the structure.

The strategy aims to modulate thermal conductivity by exciting targeted phonon modes in a quantum manner, as illustrated in Figure 1a. First, the dominant modes for heat transport are identified utilizing first-principles and molecular dynamics (MD) simulations. Then, the energy of these modes is artificially increased, allowing for the quantum excitation of dominant phonons with large contributions to thermal conductivity and weak coupling with other phonons. This results in a significant enhancement of the thermal conductivity. On the other hand, if phonons with high scattering rates and relatively low contributions to thermal conductivity are excited, scattering processes are promoted, leading to a decrease in thermal conductivity. Phonon DOS determines the number of excited modes around a specific frequency, thus indicating the effectiveness of activating those modes. It is worth noting that thermal conductivity can be modulated over a wide range by exciting only a few dominant phonons without introducing other scattering mechanisms.

The method basically relies on the nature of phonon scattering. Heat conduction in solids is directly related to phonon scattering, where an individual mode can participate in various scattering processes. By identifying the characteristic time of phonon relaxation time or lifetime, τ , the thermal conductivity can be generally written as an integration as^{9,10,24}

$$\kappa = \frac{1}{3} \int C(\omega) v^2(\omega) \tau(\omega) d\omega \quad (1)$$

where the parameter 1/3 is related to the dimension of the system, $C(\omega)$ refers to the spectral volumetric specific heat, v refers to the phonon group velocity, and ω is the frequency. In general, the diverse scatterings can be incorporated into Matthiessen’s rule^{9,24}

$$\frac{1}{\tau} = \frac{1}{\tau_{\text{ph-ph}}} + \frac{1}{\tau_{\text{im}}} + \frac{1}{\tau_{\text{b}}} \quad (2)$$

where $\tau_{\text{ph-ph}}$, τ_{im} , and τ_{b} are the relaxation times due to phonon–phonon, impurity, and boundary scattering processes, respectively. The relaxation time of phonon–phonon scattering is calculated using Fermi’s golden rule,⁷³ while impurity

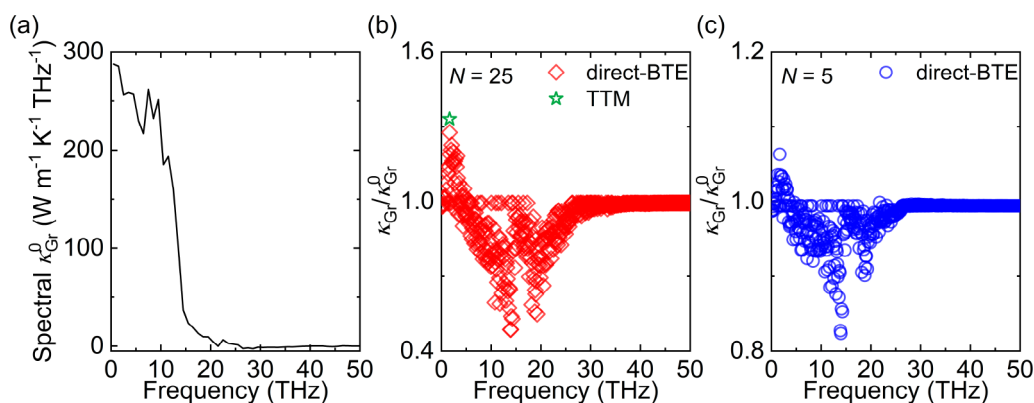


Figure 2. Thermal conductivity modulation for graphene via targeted phonon excitation. (a) Spectral contributions to k_{Gr}^0 as a function of frequency. (b, c) The relative overall thermal conductivity of graphene after and before the excitation $k_{\text{Gr}}/k_{\text{Gr}}^0$ as a function of the center frequency for targeted phonons. For instance, the first center frequency is 0.05 THz, and a few modes in 0–0.1 THz are excited with a 25 or 5 times larger energy. The energy needed for the excitation is at most 20.8 mJ m^{-2} ($N = 25$) or 3.5 mJ m^{-2} ($N = 5$).

scattering can be attained based on Klemens' derivation.⁹ In addition, crystal boundary scattering is determined by diffuse boundary absorption/emission, which depends on the Casimir length. It is important to note that impurity and boundary scatterings are not included in the calculation of this work.

By increasing the energy of targeted phonons, the scattering rate can be changed significantly, leading to modulation of the thermal conductivity. To change the energy of mode n , the phonon occupation numbers are modified in ab initio calculations according to the formulation

$$E'_n = \hbar\omega_n \frac{N}{e^{\hbar\omega_n/k_B T} - 1} \quad (3)$$

where E'_n corresponds to the energy of mode n after the modification, \hbar denotes the reduced Planck constant, k_B is the Boltzmann constant, T is the absolute lattice temperature, and N represents the multiple of energy increase.

In MD simulations, the value of N can be calculated as $\langle E'_n \rangle / \langle E_n \rangle$, which is the ratio of the mode energy after and before excitations. It is difficult to directly increase the mode energy to N times its original value in the simulation. Therefore, the atomic velocities (kinetic energy) are chosen to be rescaled according to the formulation (derivation in Appendix C in the Supporting Information)

$$v'_j = v_j + \frac{1}{\sqrt{m_j}}(\sqrt{M} - 1)\dot{Q}_n(t)e_{j,n} \quad (4)$$

where v'_j and v_j are the velocities of atom j after and before excitations, respectively, m_j is the atomic mass, \dot{Q}_n is the normal mode velocity coordinate, and $e_{j,n}$ is the eigenvector. Equation 4 implies that the mode kinetic energy $E_{n,K}$ is increased by M times. The rescale factor M is set to 10. Due to the conversion between kinetic and potential energy, as well as the evolution and diffusion, the actual multiple of energy increase N is around one-third of M (depicted in Figure S10).

The effectiveness of the strategy is demonstrated in both graphene and graphene nanoribbon systems. However, it is worth noting that this approach could be applicable to other systems with weak-coupling phonons.^{26–28} Ab initio calculations (details in Appendix A in the Supporting Information) for graphene are performed using the Vienna ab initio simulation package (VASP),⁷⁴ and the phonon transport properties are obtained by solving the phonon Boltzmann

transport equation with the special version of ShengBTE packages modified by Ruan et al., which has better convergence over two-dimensional materials,^{75,76} assisted by the PHONOPY package.⁷⁷ Additionally, nonequilibrium molecular dynamics (NEMD, details in Appendix B in the Supporting Information) simulations for graphene nanoribbon are conducted using the LAMMPS package.⁷⁸

Indeed, the specific implementation of this strategy in experimental settings is also an important and notable consideration. The selection of appropriate excitation methods depends on the specific phonons that are being targeted. Here are some brief descriptions to provide further clarity. In the case of optical phonons, for instance, they can be effectively excited by illuminating the sample with THz pulses using a tabletop light source, which are generated by optical rectification using the tilted-pulse-intensity-front scheme. The intensity of the THz pulse can be controlled by a pair of wire grid polarizers operating in the THz frequency region, as described in ref 60. Ideally, the frequency of the illuminated photons should be close to the THz magnitude, corresponding to the “targeted phonons” indicated in the thermal conductivity spectrum in Figure 2a. Techniques such as THz time domain spectroscopy (THz-TDS) can be utilized to detect any enhanced signal caused by external stimuli and compare it to the baseline (no shining) performance. Besides, in the study by Wu et al.,⁷⁹ an out-of-plane acoustic phonon is selectively excited in graphene by a different approach, scanning tunneling spectroscopy. To this end, the tunneling current was passed through a molecule adsorbed on graphene on a metal surface. The rich structure observed in the experimental inelastic electron tunneling spectra could be reproduced by nonequilibrium transport calculations. Importantly, besides the presence of spectroscopic signals due to molecular vibrational quanta, graphene phonon excitation also left its footprint in the spectra, too. This showed that the coupling of symmetry-equivalent and energetically similar vibrational modes of the molecule and graphene led to the selective excitation of a specific acoustic graphene phonon, which without the molecule remained below the detection limit. Therefore, these recent experimental findings are very encouraging and pave the way for selectively exciting targeted phonons.

First, the spectral contribution to intrinsic thermal conductivity of graphene k_{Gr}^0 is calculated as a guidance to

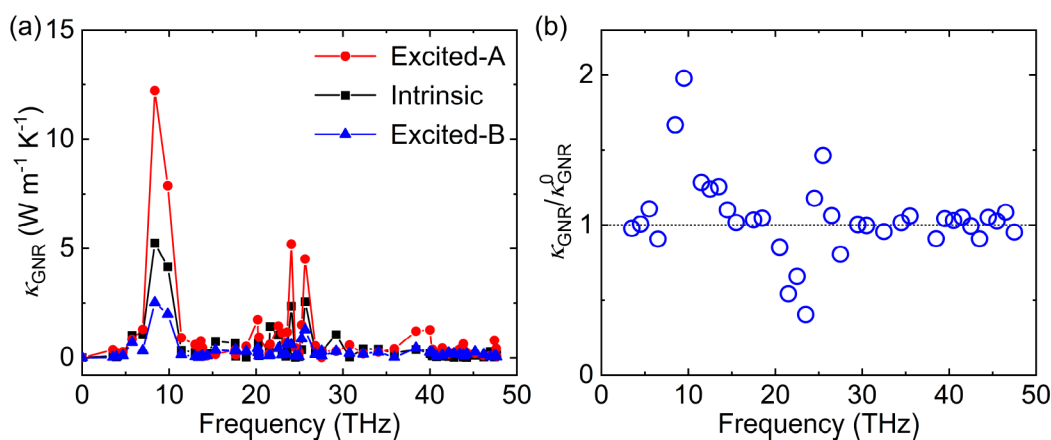


Figure 3. Thermal conductivity modulation for graphene nanoribbon (GNR) via targeted excitation of phonons. (a) Thermal conductivity contribution spectrum by molecular dynamics simulations, “A” refers to the case where two modes, 9.84 THz, $k = (-0.64, 0.96, 0)$ and 9.84 THz, $k = (0.64, -0.96, 0)$, are excited with a 3.34 times larger kinetic energy ($N = 3.34$), and “B” represents the case where four modes, 23.59 THz, $k = (-0.64, 0.37, 0)$, 23.41 THz, $k = (-0.64, 0.66, 0)$, 23.41 THz, $k = (0.64, -0.66, 0)$, and 23.59 THz, $k = (0.64, -0.37, 0)$, are excited with $N = 2.71$. k represents the wave vector. (b) Relative thermal conductivity of the graphene nanoribbon after and before the excitation $\kappa_{\text{GNR}}/\kappa_{\text{GNR}}^0$ by exciting a few modes in each 1 THz frequency range utilizing molecular dynamics simulations.

highlight the effectiveness of the modulation strategy, as shown in Figure 2a. An iterative solving method is utilized to accurately solve the Boltzmann transport equation.⁷⁵ The obtained value for k_{Gr}^0 at 300 K is $3189 \text{ W m}^{-1} \text{ K}^{-1}$, which is comparable to those in previous works ($1500\text{--}4000 \text{ W m}^{-1} \text{ K}^{-1}$).^{80–84} Figure 2a suggests that the low-frequency modes dominate the heat conduction in graphene, particularly those below 5 THz and around 10 THz. The spectral k_{Gr}^0 decreases drastically in the higher frequency range, indicating a negligible contribution of these modes to heat conduction. This observation provides a prominent information for selecting the modes to be adjusted in energy.

Then, the energy is injected to excite more heat carriers into the dominant modes. However, it can be observed from Figure 2b that the results do not correspond perfectly to the tendency shown in Figure 2a, since the DOS and scattering rates are also essential factors in implementing the modification, as illustrated in Figure 1b. The DOS determines the number of modes that can be affected during excitation, while a high scattering rate means that the modes are strongly scattered, leading to a smaller contribution to heat conduction and a larger resistance of other modes. In graphene, ZA modes play a much more significant role in heat conduction due to the symmetry-based selection rule.⁸³ The reflection symmetry of its 2D structure excludes all the 3-phonon scatterings that involve odd numbers of flexural phonons, causing a profound reduction in the scattering rates of flexural modes, especially ZA modes. Thus, exciting those modes can generate more noticeable effects. As a result, the peak of $k_{\text{Gr}}/k_{\text{Gr}}^0$ located at around 1.7 THz (k_{Gr} is the thermal conductivity of graphene after excitation) ensures a high enough DOS and a low scattering rate, as well as a high spectral thermal conductivity. On the other hand, the trough is situated around 13.9 THz, close to the maximum frequency of the ZA phonon branch, ensuring a high enough DOS, a relatively high scattering rate, and small spectral thermal conductivity compared to other ZA modes. The scattering rates’ changes after and before the excitation are also presented in Appendix A in the Supporting Information.

An alternative method has been incorporated to validate the modulation results obtained by the previously discussed direct-

BTE method. This alternative approach is termed the two-temperature model (TTM), which considers the nonequilibrium between the excited phonon group and the intrinsic phonon group (details in Appendix D in the Supporting Information). The two-temperature model is widely utilized to address weak coupling systems, including electron–phonon, phonon–phonon, and phonon–magnon couplings.^{25,26,85,86} To streamline the calculations, it is valuable to focus specifically on the peak case to avoid redundancy. It is notable that the results obtained using the two-temperature model closely correspond to those from the previous method, and interestingly, the two-temperature model demonstrates an even more pronounced modulation effect.

Molecular dynamics simulations are conducted on graphene nanoribbons to validate the feasibility of the modulation strategy, especially considering high-order scatterings. As shown in Figure 3a, the thermal conductivity contribution spectra of graphene nanoribbon ($24.9 \times 21.6 \text{ \AA}^2$) are extracted through NEMD simulations.^{87,88} The intrinsic thermal conductivity of graphene nanoribbon k_{GNR}^0 at 300 K is $59.0 \text{ W m}^{-1} \text{ K}^{-1}$, which is consistent with previous studies.⁴⁹ Due to the limitation in the simulation cell size, the possible excited phonons have smaller wavelengths and higher frequencies (above 3 THz). The thermal conductivity contribution spectrum is obtained by extracting time-dependent atomic motion data in the intermediate region where the temperature difference remains small ($<0.3 \text{ K}$ in all the cases) to ensure the validity of the lattice dynamic method. The excitation region is chosen to be all parts of the simulation cell except for the heat sink and fixed region, with the additional heat flux generated by the excitation being relatively small (2–5%) compared to the heat flux generated by the Langevin thermostat (Figure S11 in Appendix B in the Supporting Information). The excitation is conducted every 100 fs with an equivalent input energy density of $0.21\text{--}0.48 \text{ mJ m}^{-2}$. The overall thermal conductivity refers to an effective quantity measuring heat flux. It should also be noted that there are only a few modes in each 1 THz frequency range, which accounts for 2–7% of all modes of the Brillouin zone. Moreover, modes around 10 THz make a significant contribution to the intrinsic thermal conductivity, as shown in Figure 3a. In particular, selecting two modes between 9 and 10

THz as targeted phonons (excited-A) results in a considerable increase in the overall thermal conductivity, with a 97.8% enhancement (from 59.0 to 116.7 W m⁻¹ K⁻¹) when those modes are excited with $N = 3.34$ (3.34 times larger kinetic energy). Figure 3a also shows the thermal conductivity contribution after the excitation. It can be concluded that the increase of k_{GNR} (the thermal conductivity of graphene nanoribbon after excitation) is mainly contributed from modes below 10 THz and modes in the 24–26 THz range, with the contribution of these modes not changing significantly compared to the original value. Furthermore, targeted phonons in other frequency ranges are also excited in a similar manner, as shown in Figure 3b. The excitation of these modes regulates the overall thermal conductivity by different ratios. The modes between 9 and 10 THz show the highest modulation ratio, owing to high contribution to k_{GNR} , with the modes in the 25–26 THz range showing similar behavior. In general, the enhancement of k_{GNR} decreases with increasing frequency (below 15 THz). This can be attributed to higher phonon density of states (DOS) in the high-frequency range.

The modulation results of NEMD simulations for decreasing k_{GNR} exhibit a tendency similar to that of the ab initio calculations. In Figure 3a, modes in the 15–24 THz range show low contribution to k_{GNR} . When four modes between 23 and 24 THz are excited with a 2.71 times larger kinetic energy (excited-B, $N = 2.71$), k_{GNR} decreases by 59.6% (from 59.0 to 23.8 W m⁻¹ K⁻¹). The comparison before and after the excitation is shown in Figure 3a. The contribution of modes to k_{GNR} decreases over a wide frequency range with a greater reduction below 10 THz due to the large original contribution values. Additionally, exciting the modes in the frequencies between 20 and 24 THz also reduces k_{GNR} (from 85.1% to 40.4%), as illustrated in Figure 3b. The reduction of k_{GNR} is significant and decreases as the frequency of targeted phonons increases (below 24 THz). This trend can be related to high intrinsic scattering rates and low phonon DOS of modes around 23 THz compared to other modes.

Generally, the thermal conductivity of dielectric materials can be finely tuned based on the specific characteristics of phonon transport. For example, the introduction of ¹³C can result in roughly a 50% reduction in thermal conductivity compared to isotopically pure graphene, attributed to strong phonon-point defect scattering.⁸⁹ In the case of graphene nanoribbons, phonon transport can be hindered by local resonant hybridization from nanostructures on the sides, leading to a 73% reduction in thermal conductivity.⁴⁹ Additionally, strain can alter thermal transport properties by affecting the morphology. For instance, when the compressive strain reaches 0.08, the thermal conductivity of graphene decreases by about 45% due to structural buckling.⁹⁰ While these methods can achieve considerable regulatory results, they are not in situ and require structural modification or deformation. Comparatively, the targeted phonon excitation strategy can not only effectively reduce thermal conductivity but also represent a very promising direction for enhancing thermal transport in addition to reducing impurity scattering.

Defects in materials, such as impurities or isotopes, also have a crucial effect on the regulation results. The effect of targeted phonon excitation is contingent upon a competitive mechanism, which induces changes in the scattering rates and heat transfer pathways. When defect scattering is introduced, the intrinsic thermal conductivity can be reduced. Then, both the modulation results in the peak and trough cases after excitation

might decrease. In analytical models, the phonon-defect scattering rate is typically approximated as $\sim\omega^{4,91}$ exhibiting a less pronounced frequency dependence in graphene.^{92,93} This implies that higher frequency phonons experience stronger scattering compared to lower frequency phonons. Consequently, the peak in the thermal conductivity modulation might shift toward lower frequencies, while the trough might shift toward higher frequencies. Nevertheless, the overall trend of regulation remains unchanged. Besides, other types of scattering work in a similar way, e.g., boundary scattering. Therefore, the introduction of defect scattering does not alter the overall trend of relative thermal conductivity concerning the frequency of targeted phonons. But it affects the specific modulation range, as well as the positions of the peak and trough.

In this work, a new strategy for modulating thermal conductivity is proposed that is realized by exciting targeted phonons in a quantum manner. The results demonstrate that this strategy can effectively modulate the thermal conductivity of graphene and graphene nanoribbons over a wide range compared to their intrinsic values. Ab initio calculations and NEMD simulations provide detailed validation for the strategy. First, the modes with top-contribution or strong-scattering are identified; then, the energy of some of these modes is artificially increased. It is worth noting that the feasibility of this strategy has a high possibility to be confirmed experimentally.^{60,61,70,79} This is because the quantum excitation of vibrational modes has already been used to modulate transport properties and induce structural phase transitions.^{61,67,68,70}

This strategy represents a substantial advancement in modulating thermal conductivity/heat flux among various dielectric materials. More profoundly, it significantly contributes to the understanding of phonon transport in low-dimensional systems. And targeted phonon excitation holds crucial significance for the thermal management of electronic devices, while also paving the way for the development of thermal functional devices. In addition, by substantially reducing the thermal conductivity, it offers a novel avenue to enhance thermoelectric efficiency.

■ ASSOCIATED CONTENT

Supporting Information

The Supporting Information is available free of charge at <https://pubs.acs.org/doi/10.1021/acs.nanolett.4c00478>.

Additional ab initio calculation details, molecular dynamics simulation setup, derivation of the velocity rescaling formula, and derivation of the two-temperature model (PDF)

■ AUTHOR INFORMATION

Corresponding Author

Nuo Yang — School of Energy and Power Engineering, Huazhong University of Science and Technology, Wuhan 430074, People's Republic of China; Department of Physics, National University of Defense Technology, Changsha 410073, People's Republic of China; orcid.org/0000-0003-0973-1718; Email: nuo@hust.edu.cn, nuo@nudt.edu.cn

Authors

- Xiao Wan – School of Energy and Power Engineering, Huazhong University of Science and Technology, Wuhan 430074, People's Republic of China
- Dongkai Pan – School of Energy and Power Engineering, Huazhong University of Science and Technology, Wuhan 430074, People's Republic of China
- Zhicheng Zong – School of Energy and Power Engineering, Huazhong University of Science and Technology, Wuhan 430074, People's Republic of China
- Yangjun Qin – School of Energy and Power Engineering, Huazhong University of Science and Technology, Wuhan 430074, People's Republic of China
- Jing-Tao Lü – School of Physics and Wuhan National High Magnetic Field Center, Huazhong University of Science and Technology, Wuhan 430074, People's Republic of China
- Sebastian Volz – LIMMS, CNRS-IIS UMI 2820, The University of Tokyo, Tokyo 153-8505, Japan; Institute of Industrial Science, The University of Tokyo, Tokyo 153-8505, Japan
- Lifa Zhang – Phonon Engineering Research Center of Jiangsu Province, Ministry of Education Key Laboratory of NSLSCS, Center for Quantum Transport and Thermal Energy Science, Institute of Physics Frontiers and Interdisciplinary Sciences, School of Physics and Technology, Nanjing Normal University, Nanjing 210023, People's Republic of China; orcid.org/0000-0001-6108-1404

Complete contact information is available at:

<https://pubs.acs.org/10.1021/acs.nanolett.4c00478>

Author Contributions

[†]X.W. and D.P. contributed equally to this work.

Notes

The authors declare no competing financial interest.

ACKNOWLEDGMENTS

This work was sponsored by the National Key Research and Development Project of China, No. 2018YFE0127800. We are grateful to Jörg Kröger, Zhengyou Liu, Junichiro Shiomi, Shouhang Li, Wu Li, Xiaokun Gu, and Lina Yang for helpful discussions. The authors thank the National Supercomputing Center in Tianjin (NSCC-TJ) and the China Scientific Computing Grid (ScGrid) for providing assistance in computations.

REFERENCES

- (1) Qian, X.; Zhou, J.; Chen, G. Phonon-engineered extreme thermal conductivity materials. *Nat. Mater.* **2021**, *20*, 1188–1202.
- (2) Huang, C.; Qian, X.; Yang, R. Thermal conductivity of polymers and polymer nanocomposites. *Materials Science and Engineering: R: Reports* **2018**, *132*, 1–22.
- (3) Xu, X.; Chen, J.; Zhou, J.; Li, B. Thermal Conductivity of Polymers and Their Nanocomposites. *Adv. Mater.* **2018**, *30* (17), 1705544.
- (4) Mao, J.; Chen, G.; Ren, Z. Thermoelectric cooling materials. *Nat. Mater.* **2021**, *20* (4), 454–461.
- (5) Dresselhaus, M. S.; Chen, G.; Tang, M. Y.; Yang, R. G.; Lee, H.; Wang, D. Z.; Ren, Z. F.; Fleurial, J. P.; Gogna, P. New Directions for Low-Dimensional Thermoelectric Materials. *Adv. Mater.* **2007**, *19* (8), 1043–1053.
- (6) Cahill, D. G.; Braun, P. V.; Chen, G.; Clarke, D. R.; Fan, S.; Goodson, K. E.; Keblinski, P.; King, W. P.; Mahan, G. D.; Majumdar, A.; Maris, H. J.; Phillpot, S. R.; Pop, E.; Shi, L. Nanoscale thermal

- transport, II. 2003–2012. *Applied Physics Reviews* **2014**, *1* (1), 011305.
- (7) Allen, P. B.; Feldman, J. L. Thermal conductivity of disordered harmonic solids. *Phys. Rev. B* **1993**, *48* (17), 12581–12588.
- (8) Dove, M. T. *Introduction to Lattice Dynamics*; Cambridge University Press: 1993.
- (9) Chen, G. *Nanoscale energy transport and conversion: a parallel treatment of electrons, molecules, phonons, and photons*; Oxford University Press: 2005.
- (10) Kittel, C. *Introduction to solid state physics*, 7th ed.; Wiley: 1996.
- (11) Chen, G. Non-Fourier phonon heat conduction at the microscale and nanoscale. *Nature Reviews Physics* **2021**, *3* (8), 555–569.
- (12) Chen, G.; Zeng, T.; Borca-Tasciuc, T.; Song, D. Phonon engineering in nanostructures for solid-state energy conversion. *Materials Science and Engineering: A* **2000**, *292* (2), 155–161.
- (13) Li, N.; Ren, J.; Wang, L.; Zhang, G.; Hänggi, P.; Li, B. Colloquium: Phononics: Manipulating heat flow with electronic analogs and beyond. *Rev. Mod. Phys.* **2012**, *84* (3), 1045–1066.
- (14) Gu, X.; Wei, Y.; Yin, X.; Li, B.; Yang, R. Colloquium: Phononic thermal properties of two-dimensional materials. *Rev. Mod. Phys.* **2018**, *90* (4), 041002.
- (15) Liu, Y.; Ren, W.; An, M.; Dong, L.; Gao, L.; Shai, X.; Wei, T.; Nie, L.; Hu, S.; Zeng, C. A Qualitative Study of the Disorder Effect on the Phonon Transport in a Two-Dimensional Graphene/h-BN Heterostructure. *Frontiers in Materials* **2022**, *9*, 913764.
- (16) Zhu, G.-p.; Zhao, C.-w.; Wang, X.-w.; Wang, J. Tuning Thermal Conductivity in Si Nanowires with Patterned Structures. *Chin. Phys. Lett.* **2021**, *38* (2), 024401.
- (17) Lindsay, L.; Broido, D. A.; Reinecke, T. L. First-Principles Determination of Ultrahigh Thermal Conductivity of Boron Arsenide: A Competitor for Diamond? *Phys. Rev. Lett.* **2013**, *111* (2), 025901.
- (18) Kang, J. S.; Li, M.; Wu, H.; Nguyen, H.; Hu, Y. Experimental observation of high thermal conductivity in boron arsenide. *Science* **2018**, *361* (6402), 575–578.
- (19) Li, S.; Zheng, Q.; Lv, Y.; Liu, X.; Wang, X.; Huang, P. Y.; Cahill, D. G.; Lv, B. High thermal conductivity in cubic boron arsenide crystals. *Science* **2018**, *361* (6402), 579–581.
- (20) Tian, F.; Song, B.; Chen, X.; Ravichandran, N. K.; Lv, Y.; Chen, K.; Sullivan, S.; Kim, J.; Zhou, Y.; Liu, T.-H.; Goni, M.; Ding, Z.; Sun, J.; Udalamatta Gamage, G. A. G.; Sun, H.; Ziyae, H.; Huyan, S.; Deng, L.; Zhou, J.; Schmidt, A. J.; Chen, S.; Chu, C.-W.; Huang, P. Y.; Broido, D.; Shi, L.; Chen, G.; Ren, Z. Unusual high thermal conductivity in boron arsenide bulk crystals. *Science* **2018**, *361* (6402), 582.
- (21) Kim, W. Strategies for engineering phonon transport in thermoelectrics. *Journal of Materials Chemistry C* **2015**, *3* (40), 10336–10348.
- (22) Feng, T.; Qiu, B.; Ruan, X. Coupling between phonon-phonon and phonon-impurity scattering: A critical revisit of the spectral Matthiessen's rule. *Phys. Rev. B* **2015**, *92* (23), 235206.
- (23) Liu, Z.; Mao, J.; Liu, T.-H.; Chen, G.; Ren, Z. Nano-microstructural control of phonon engineering for thermoelectric energy harvesting. *MRS Bull.* **2018**, *43* (3), 181–186.
- (24) Tien, C. L. *Microscale energy transfer*; CRC Press: 1997.
- (25) Chen, J.; Xu, X.; Zhou, J.; Li, B. Interfacial thermal resistance: Past, present, and future. *Rev. Mod. Phys.* **2022**, *94* (2), 025002.
- (26) An, M.; Song, Q.; Yu, X.; Meng, H.; Ma, D.; Li, R.; Jin, Z.; Huang, B.; Yang, N. Generalized Two-Temperature Model for Coupled Phonons in Nanosized Graphene. *Nano Lett.* **2017**, *17* (9), 5805–5810.
- (27) Deng, C.; Huang, Y.; An, M.; Yang, N. Phonon weak couplings model and its applications: A revisit to two-temperature non-equilibrium transport. *Materials Today Physics* **2021**, *16*, 100305.
- (28) Pan, D.; Zong, Z.; Yang, N. Phonon weak couplings in nanoscale thermophysics. *Acta Physica Sinica* **2022**, *71* (8), 086302.
- (29) Lee, S.; Broido, D.; Esfarjani, K.; Chen, G. Hydrodynamic phonon transport in suspended graphene. *Nat. Commun.* **2015**, *6* (1), 6290.

- (30) Callaway, J. Model for Lattice Thermal Conductivity at Low Temperatures. *Phys. Rev.* **1959**, *113* (4), 1046–1051.
- (31) Hu, S.; An, M.; Yang, N.; Li, B. Manipulating the temperature dependence of the thermal conductivity of graphene phononic crystal. *Nanotechnology* **2016**, *27* (26), 265702.
- (32) Fang, T.; Konar, A.; Xing, H.; Jena, D. Mobility in semiconducting graphene nanoribbons: Phonon, impurity, and edge roughness scattering. *Phys. Rev. B* **2008**, *78* (20), 205403.
- (33) Yang, N.; Zhang, G.; Li, B. Violation of Fourier's law and anomalous heat diffusion in silicon nanowires. *Nano Today* **2010**, *5* (2), 85–90.
- (34) Liao, Q.; Liu, Z.; Liu, W.; Deng, C.; Yang, N. Extremely High Thermal Conductivity of Aligned Carbon Nanotube-Polyethylene Composites. *Sci. Rep.* **2015**, *5* (1), 16543.
- (35) Barbalinardo, G.; Chen, Z.; Dong, H.; Fan, Z.; Donadio, D. Ultrahigh Convergent Thermal Conductivity of Carbon Nanotubes from Comprehensive Atomistic Modeling. *Phys. Rev. Lett.* **2021**, *127* (2), 025902.
- (36) Deng, S.; Ma, D.; Zhang, G.; Yang, N. Modulating the thermal conductivity of crystalline nylon by tuning hydrogen bonds through structure poling. *Journal of Materials Chemistry A* **2021**, *9* (43), 24472–24479.
- (37) Deng, S.; Yuan, J.; Lin, Y.; Yu, X.; Ma, D.; Huang, Y.; Ji, R.; Zhang, G.; Yang, N. Electric-field-induced modulation of thermal conductivity in poly(vinylidene fluoride). *Nano Energy* **2021**, *82*, 105749.
- (38) Yu, X.; Ma, D.; Deng, C.; Wan, X.; An, M.; Meng, H.; Li, X.; Huang, X.; Yang, N. How Does van der Waals Confinement Enhance Phonon Transport? *Chin. Phys. Lett.* **2021**, *38* (1), 014401.
- (39) Dames, C. Ultrahigh thermal conductivity confirmed in boron arsenide. *Science* **2018**, *361* (6402), 549–550.
- (40) van Rookeghem, A.; Carrete, J.; Oses, C.; Curtarolo, S.; Mingo, N. High-Throughput Computation of Thermal Conductivity of High-Temperature Solid Phases: The Case of Oxide and Fluoride Perovskites. *Physical Review X* **2016**, *6* (4), 041061.
- (41) Henry, A.; Chen, G. High Thermal Conductivity of Single Polyethylene Chains Using Molecular Dynamics Simulations. *Phys. Rev. Lett.* **2008**, *101* (23), 235502.
- (42) Shen, S.; Henry, A.; Tong, J.; Zheng, R.; Chen, G. Polyethylene nanofibres with very high thermal conductivities. *Nat. Nanotechnol.* **2010**, *5* (4), 251–255.
- (43) Katre, A.; Carrete, J.; Dongre, B.; Madsen, G. K. H.; Mingo, N. Exceptionally Strong Phonon Scattering by B Substitution in Cubic SiC. *Phys. Rev. Lett.* **2017**, *119* (7), 075902.
- (44) Yamawaki, M.; Ohnishi, M.; Ju, S.; Shiomi, J. Multifunctional structural design of graphene thermoelectrics by Bayesian optimization. *Science Advances* **2018**, *4* (6), No. eaar4192.
- (45) An, M.; Li, L.; Hu, S.; Ding, Z.; Yu, X.; Demir, B.; Yang, N.; Ma, W.; Zhang, X. Mass difference and polarization lead to low thermal conductivity of graphene-like carbon nitride (C₃N). *Carbon* **2020**, *162*, 202–208.
- (46) An, M.; Wang, H.; Yuan, Y.; Chen, D.; Ma, W.; Sharshir, S. W.; Zheng, Z.; Zhao, Y.; Zhang, X. Strong phonon coupling induces low thermal conductivity of one-dimensional carbon boron nanotube. *Surfaces and Interfaces* **2022**, *28*, 101690.
- (47) Ma, D.; Arora, A.; Deng, S.; Xie, G.; Shiomi, J.; Yang, N. Quantifying phonon particle and wave transport in silicon nanophononic metamaterial with cross junction. *Materials Today Physics* **2019**, *8*, 56–61.
- (48) Yang, L.; Yang, N.; Li, B. Extreme Low Thermal Conductivity in Nanoscale 3D Si Phononic Crystal with Spherical Pores. *Nano Lett.* **2014**, *14* (4), 1734–1738.
- (49) Ma, D.; Wan, X.; Yang, N. Unexpected thermal conductivity enhancement in pillared graphene nanoribbon with isotopic resonance. *Phys. Rev. B* **2018**, *98* (24), 245420.
- (50) Hussein, M. I.; Tsai, C.-N.; Honarvar, H. Thermal Conductivity Reduction in a Nanophononic Metamaterial versus a Nanophononic Crystal: A Review and Comparative Analysis. *Adv. Funct. Mater.* **2020**, *30* (8), 1906718.
- (51) Wan, X.; Ma, D.; Pan, D.; Yang, L.; Yang, N. Optimizing thermal transport in graphene nanoribbons based on phonon resonance hybridization. *Materials Today Physics* **2021**, *20*, 100445.
- (52) Zhang, Z.; Guo, Y.; Bescond, M.; Chen, J.; Nomura, M.; Volz, S. Heat Conduction Theory Including Phonon Coherence. *Phys. Rev. Lett.* **2022**, *128* (1), 015901.
- (53) An, M.; Chen, D.; Ma, W.; Hu, S.; Zhang, X. Directly visualizing the crossover from incoherent to coherent phonons in two-dimensional periodic MoS₂/MoSe₂ arrayed heterostructure. *Int. J. Heat Mass Transfer* **2021**, *178*, 121630.
- (54) Ma, D.; Ding, H.; Meng, H.; Feng, L.; Wu, Y.; Shiomi, J.; Yang, N. Nano-cross-junction effect on phonon transport in silicon nanowire cages. *Phys. Rev. B* **2016**, *94* (16), 165434.
- (55) Davis, B. L.; Hussein, M. I. Nanophononic Metamaterial: Thermal Conductivity Reduction by Local Resonance. *Phys. Rev. Lett.* **2014**, *112* (5), 055505.
- (56) Xu, Z.; Baowen, L. Phonon condensation and cooling via nonlinear feedback (2022-01-01); arXiv:2201.00251.
- (57) Xu, Y.; Kraemer, D.; Song, B.; Jiang, Z.; Zhou, J.; Loomis, J.; Wang, J.; Li, M.; Ghasemi, H.; Huang, X.; Li, X.; Chen, G. Nanostructured polymer films with metal-like thermal conductivity. *Nat. Commun.* **2019**, *10* (1), 1771.
- (58) Dong, L.; Xi, Q.; Zhou, J.; Xu, X.; Li, B. Phonon Renormalization Induced by Electric Field in Ferroelectric Poly(Vinylidene Fluoride-Trifluoroethylene) Nanofibers. *Physical Review Applied* **2020**, *13* (3), 034019.
- (59) Yang, L.; Zhang, Q.; Hu, G.; Yang, N. Deformation insensitive thermal conductance of the designed Si metamaterial. *Appl. Phys. Lett.* **2023**, *123* (6), 062201.
- (60) Sekiguchi, F.; Hirori, H.; Yumoto, G.; Shimazaki, A.; Nakamura, T.; Wakamiya, A.; Kanemitsu, Y. Enhancing the Hot-Phonon Bottleneck Effect in a Metal Halide Perovskite by Terahertz Phonon Excitation. *Phys. Rev. Lett.* **2021**, *126* (7), 077401.
- (61) Bakulin, A. A.; Lovrincic, R.; Yu, X.; Selig, O.; Bakker, H. J.; Rezus, Y. L. A.; Nayak, P. K.; Fonari, A.; Coropceanu, V.; Brédas, J.-L.; Cahen, D. Mode-selective vibrational modulation of charge transport in organic electronic devices. *Nat. Commun.* **2015**, *6* (1), 7880.
- (62) Price, M. B.; Butkus, J.; Jellicoe, T. C.; Sadhanala, A.; Briane, A.; Halpert, J. E.; Broch, K.; Hodgkiss, J. M.; Friend, R. H.; Deschler, F. Hot-carrier cooling and photoinduced refractive index changes in organic–inorganic lead halide perovskites. *Nat. Commun.* **2015**, *6* (1), 8420.
- (63) Yang, Y.; Ostrowski, D. P.; France, R. M.; Zhu, K.; van de Lagemaat, J.; Luther, J. M.; Beard, M. C. Observation of a hot-phonon bottleneck in lead-iodide perovskites. *Nat. Photonics* **2016**, *10* (1), 53–59.
- (64) Yang, J.; Wen, X.; Xia, H.; Sheng, R.; Ma, Q.; Kim, J.; Tapping, P.; Harada, T.; Kee, T. W.; Huang, F.; Cheng, Y.-B.; Green, M.; Ho-Baillie, A.; Huang, S.; Shrestha, S.; Patterson, R.; Conibeer, G. Acoustic-optical phonon up-conversion and hot-phonon bottleneck in lead-halide perovskites. *Nat. Commun.* **2017**, *8* (1), 14120.
- (65) Sullivan, S.; Vallabhaneni, A.; Kholmanov, I.; Ruan, X.; Murthy, J.; Shi, L. Optical Generation and Detection of Local Nonequilibrium Phonons in Suspended Graphene. *Nano Lett.* **2017**, *17* (3), 2049–2056.
- (66) Wang, R.; Zobeiri, H.; Xie, Y.; Wang, X.; Zhang, X.; Yue, Y. Distinguishing Optical and Acoustic Phonon Temperatures and Their Energy Coupling Factor under Photon Excitation in nm 2D Materials. *Advanced Science* **2020**, *7* (13), 2000097.
- (67) Guo, H.; Chu, W.; Prezhdo, O. V.; Zheng, Q.; Zhao, J. Strong Modulation of Band Gap, Carrier Mobility and Lifetime in Two-Dimensional Black Phosphorene through Acoustic Phonon Excitation. *J. Phys. Chem. Lett.* **2021**, *12* (16), 3960–3967.
- (68) Gordiz, K.; Mui, S.; Zeier, W. G.; Shao-Horn, Y.; Henry, A. Enhancement of ion diffusion by targeted phonon excitation. *Cell Reports Physical Science* **2021**, *2* (5), 100431.

- (69) Itin, A. P.; Katsnelson, M. I. Efficient excitation of nonlinear phonons via chirped pulses: Induced structural phase transitions. *Phys. Rev. B* **2018**, *97* (18), 184304.
- (70) Hase, M.; Fons, P.; Mitrofanov, K.; Kolobov, A. V.; Tominaga, J. Femtosecond structural transformation of phase-change materials far from equilibrium monitored by coherent phonons. *Nat. Commun.* **2015**, *6* (1), 8367.
- (71) Ward, A.; Broido, D. A.; Stewart, D. A.; Deinzer, G. Ab initio theory of the lattice thermal conductivity in diamond. *Phys. Rev. B* **2009**, *80* (12), 125203.
- (72) Rapaport, D. C. *The Art of Molecular Dynamics Simulation*, 2nd ed.; Cambridge University Press: 2004.
- (73) Ziman, J. M. *Electrons and phonons: the theory of transport phenomena in solids*; Oxford University Press: 2001.
- (74) Kresse, G.; Furthmüller, J. Efficient iterative schemes for ab initio total-energy calculations using a plane-wave basis set. *Phys. Rev. B* **1996**, *54* (16), 11169–11186.
- (75) Li, W.; Carrete, J.; Katcho, N. A.; Mingo, N. ShengBTE: A solver of the Boltzmann transport equation for phonons. *Comput. Phys. Commun.* **2014**, *185* (6), 1747–1758.
- (76) Han, Z.; Yang, X.; Li, W.; Feng, T.; Ruan, X. FourPhonon: An extension module to ShengBTE for computing four-phonon scattering rates and thermal conductivity. *Comput. Phys. Commun.* **2022**, *270*, 108179.
- (77) Togo, A.; Oba, F.; Tanaka, I. First-principles calculations of the ferroelastic transition between rutile-type and CaCl_2 -type SiO_2 at high pressures. *Phys. Rev. B* **2008**, *78* (13), 134106.
- (78) Plimpton, S. Fast Parallel Algorithms for Short-Range Molecular Dynamics. *J. Comput. Phys.* **1995**, *117* (1), 1–19.
- (79) Wu, X.; Néel, N.; Brandbyge, M.; Kröger, J. Enhancement of Graphene Phonon Excitation by a Chemically Engineered Molecular Resonance. *Phys. Rev. Lett.* **2023**, *130* (11), 116201.
- (80) Balandin, A. A. Thermal properties of graphene and nanostructured carbon materials. *Nat. Mater.* **2011**, *10* (8), 569–581.
- (81) Balandin, A. A.; Ghosh, S.; Bao, W.; Calizo, I.; Teweldebrhan, D.; Miao, F.; Lau, C. N. Superior Thermal Conductivity of Single-Layer Graphene. *Nano Lett.* **2008**, *8* (3), 902–907.
- (82) Cai, W.; Moore, A. L.; Zhu, Y.; Li, X.; Chen, S.; Shi, L.; Ruoff, R. S. Thermal Transport in Suspended and Supported Monolayer Graphene Grown by Chemical Vapor Deposition. *Nano Lett.* **2010**, *10* (5), 1645–1651.
- (83) Lindsay, L.; Li, W.; Carrete, J.; Mingo, N.; Broido, D. A.; Reinecke, T. L. Phonon thermal transport in strained and unstrained graphene from first principles. *Phys. Rev. B* **2014**, *89* (15), 155426.
- (84) Xu, X.; Pereira, L. F. C.; Wang, Y.; Wu, J.; Zhang, K.; Zhao, X.; Bae, S.; Tinh Bui, C.; Xie, R.; Thong, J. T. L.; Hong, B. H.; Loh, K. P.; Donadio, D.; Li, B.; Özyilmaz, B. Length-dependent thermal conductivity in suspended single-layer graphene. *Nat. Commun.* **2014**, *5* (1), 3689.
- (85) Majumdar, A.; Reddy, P. Role of electron–phonon coupling in thermal conductance of metal–nonmetal interfaces. *Appl. Phys. Lett.* **2004**, *84* (23), 4768–4770.
- (86) Liao, B.; Zhou, J.; Chen, G. Generalized Two-Temperature Model for Coupled Phonon-Magnon Diffusion. *Phys. Rev. Lett.* **2014**, *113* (2), 025902.
- (87) Zhou, Y.; Hu, M. Quantitatively analyzing phonon spectral contribution of thermal conductivity based on nonequilibrium molecular dynamics simulations. II. From time Fourier transform. *Physical Review B* **2015**, *92* (19), 195205.
- (88) Zhou, Y.; Zhang, X.; Hu, M. Quantitatively analyzing phonon spectral contribution of thermal conductivity based on nonequilibrium molecular dynamics simulations, I. From space Fourier transform. *Phys. Rev. B* **2015**, *92* (19), 195204.
- (89) Chen, S.; Wu, Q.; Mishra, C.; Kang, J.; Zhang, H.; Cho, K.; Cai, W.; Balandin, A. A.; Ruoff, R. S. Thermal conductivity of isotopically modified graphene. *Nat. Mater.* **2012**, *11* (3), 203–207.
- (90) Li, X.; Maute, K.; Dunn, M. L.; Yang, R. Strain effects on the thermal conductivity of nanostructures. *Phys. Rev. B* **2010**, *81* (24), 245318.
- (91) Kaviany, M. *Heat transfer physics*; Cambridge University Press: 2014.
- (92) Feng, T.; Ruan, X.; Ye, Z.; Cao, B. Spectral phonon mean free path and thermal conductivity accumulation in defected graphene: The effects of defect type and concentration. *Phys. Rev. B* **2015**, *91* (22), 224301.
- (93) Hu, S.; Chen, J.; Yang, N.; Li, B. Thermal transport in graphene with defect and doping: Phonon modes analysis. *Carbon* **2017**, *116*, 139–144.